

Relative Geodesics in the Special Euclidean Group

Darryl D. Holm^{*1}, Lyle Noakes^{†2}, and Joris Vankerschaver^{‡1}

¹*Department of Mathematics, Imperial College London, London SW7 2AZ, United Kingdom*

²*School of Mathematics and Statistics, The University of Western Australia, 35 Stirling Highway, Crawley WA 6009, Australia*

May 16, 2013

Abstract

We propose a notion of distance between two parametrized planar curves, called their *discrepancy*, and defined intuitively as the minimal amount of deformation needed to deform the source curve into the target curve. A precise definition of discrepancy is given as follows. A curve of transformations in the special Euclidean group $SE(2)$ is said to be *admissible* if it maps the source curve to the target curve under the point-wise action of $SE(2)$ on the plane. After endowing the group $SE(2)$ with a left-invariant metric, we define a relative geodesic in $SE(2)$ to be a critical point of the energy functional associated to the metric, over all admissible curves. The discrepancy is then defined as the value of the energy of the minimizing relative geodesic. In the first part of the paper, we derive a scalar ODE which is a necessary condition for a curve in $SE(2)$ to be a relative geodesic, and we discuss some of the properties of the discrepancy. In the second part of the paper, we consider discrete curves, and by means of a variational principle, we derive a system of discrete equations for the relative geodesics. We finish with several examples.

Contents

1	Introduction	2
2	The Euclidean Group $SE(2)$	4
3	Continuous Relative Geodesics in $SE(2)$	5
3.1	The Deformation Energy	6
3.2	The Continuous Equations of Motion	7
3.3	Discrepancy between Planar Curves	10

*Email address: d.holm@imperial.ac.uk

†Email address: lyle.noakes@uwa.edu.au

‡Email address: joris.vankerschaver@gmail.com

4	Discrete Relative Geodesics in $SE(2)$	13
4.1	The Cayley Map	13
4.2	The Deformation Energy	15
4.3	Practical Implementation of the Discrete Equations of Motion	17
4.4	Solving the Boundary Value Problem	19
5	Direct Minimization of the Energy Functional	20
6	Numerical Results	21
6.1	Discrepancy of Simple Planar Curves	21
6.2	Interpolation for Curves on $SE(2)$	22
6.3	Asymmetry of the Discrepancy	22
6.4	Discrepancy of Polynomial Curves	23
7	Conclusions and Outlook	26

1 Introduction

Historical overview. Computational anatomy is the modern study of anatomical shape and its variability. This study originated in 1917, in the seminal book *Growth and Form* by D’Arcy Thompson, who recognized that anatomical comparison is a mathematical problem, and that its solution would lie in what he called *the Theory of Transformations* [15, p1032].¹ Since then, D’Arcy Thompson has been proven correct and many mathematical concepts, particularly concepts from Lie groups, Riemannian geometry and analysis have been applied to solve what is now called “the image registration problem”. An example is the comparison of medical images, which is a world-wide technology with an enormous number of uses every day. Perhaps not surprisingly, the comparison of medical images is still based on the Theory of Transformations, as enhanced by its modern developments.

Many mathematical frameworks have been developed to deal with the image registration problem, using the Theory of Transformations. The modern frameworks are well-developed and fascinating for the geometry and analysis that underlies their solutions of the image registration problem. An outstanding example is the framework of *large deformation diffeomorphic metric mapping* (LDDMM).² Many papers and books have been written about LDDMM and its variants. We refer the reader to the fundamental texts [12, 17].

Contributions of this paper. The present work arose in the context of LDDMM, but it reformulates the problem of registration in a simple and direct manner, for the comparison of two planar curves without using the diffeomorphism group. The reformulation is based on

¹In his book, Thompson says he “learnt of it from Henri Poincaré”.

²Recall that a diffeomorphism is a smooth invertible map, with a smooth inverse.

the idea that the *discrepancy* between two planar curves could be estimated quantitatively by defining the minimal amount of deformation needed to deform the source curve into the target curve using only the transformations of the special Euclidean group $SE(2)$ of rotations and translations acting point-wise on the plane. The point of the paper is to define *discrepancy* precisely enough, that the quantitative comparison will be meaningful.

Before explaining the main content of the paper and how it is organized, we present a few definitions and notation that set the context.

Let $\mathbf{c}_0, \mathbf{c}_1 : [0, 1] \rightarrow M$ be C^∞ curves, where M is a C^∞ manifold. Let G be a Lie group with a Riemannian metric $\langle \cdot, \cdot \rangle$, and a transitive left action \cdot on M . A C^∞ function $g : [0, 1] \rightarrow G$ is called *admissible* when $g(s) \cdot \mathbf{c}_0(s) = \mathbf{c}_1(s)$ for all $s \in [0, 1]$. The *energy* of an admissible g is

$$E_0(g) := \frac{1}{2} \int_0^1 \|g'(s)\|_{g(s)}^2 ds$$

where $\|\cdot\|_{g(s)}$ denotes the Riemannian norm. A critical point g of E_0 is said to be a *geodesic relative to $\mathbf{c}_0, \mathbf{c}_1$* , or just a *relative geodesic* when $\mathbf{c}_0, \mathbf{c}_1$ are understood.

The present paper investigates relative geodesics in the special case where G is the group $SE(2)$ of Euclidean motions of \mathbb{R}^2 , with a particular kind of left-invariant Riemannian metric, and the standard left action on $M = \mathbb{R}^2$. Then, given $\mathbf{c}_0, \mathbf{c}_1 : [0, 1] \rightarrow \mathbb{R}^2$, their *discrepancy* $\delta(\mathbf{c}_0, \mathbf{c}_1)$ is the minimum of $E_0(g)$ as g varies over all admissible curves in $SE(2)$. A minimiser g of E_0 is necessarily a relative geodesic although, as seen in Proposition 3.8, not all relative geodesics are minimisers.

When the discrepancy is 0 there is a constant admissible g , namely $\mathbf{c}_0, \mathbf{c}_1$ are congruent. More generally the minimum energy $\delta(\mathbf{c}_0, \mathbf{c}_1)$ is the minimum total variability of an admissible g . This is meant to capture, to some degree, the intuitive difficulty we find in transforming by eye from the parametric curve \mathbf{c}_0 to \mathbf{c}_1 .

Because the Riemannian metric on $SE(2)$ is chosen to be left-invariant, it follows easily that $\delta(\mathbf{c}_0, h \cdot \mathbf{c}_1) = \delta(\mathbf{c}_0, \mathbf{c}_1)$ for any constant $h \in G$. Usually however $\delta(h \cdot \mathbf{c}_0, \mathbf{c}_1) \neq \delta(\mathbf{c}_0, \mathbf{c}_1)$. Indeed usually $\delta(\mathbf{c}_0, \mathbf{c}_1) \neq \delta(\mathbf{c}_1, \mathbf{c}_0)$, as in Proposition 3.7. Sometimes there are continua of relative geodesics, as in Lemmas 3.5, 3.6. These facts are found by studying the Euler-Lagrange equations (called the continuous equations of motion) for relative geodesics, together with the natural boundary conditions at $s = 0, 1$. The Euler-Lagrange equations for relative geodesics are derived in §3 by Euler-Poincaré reduction, and also directly.

In §4 we introduce discrete analogues of relative geodesics in $SE(2)$, as objects of separate interest, and with a view to developing numerical methods for continuous relative geodesics. Discrete curves are finite sequences, and the discrete energy is defined in terms of the Cayley map for $SE(2)$. The Euler-Poincaré approach adapts nicely to the discrete case, leading to projected discrete equations of motion (47), and projected discrete boundary conditions (48), from which discrete relative geodesics can be found by Newton iteration. Alternatively, discrete relative geodesics can be calculated by direct minimisation of the discrete energy. In §6 the numerical methods developed in §4 are used to illustrate properties of relative geodesics and discrepancies for some simple examples of plane curves. A morphing procedure, using a minimal relative geodesic, illustrates the geometrical difficulty of transforming \mathbf{c}_0 to \mathbf{c}_1 .

2 The Euclidean Group $SE(2)$

In this section, we recall some basic results about the Lie group $SE(2)$, which consists of rotations and translations in the Euclidean plane. For more information about $SE(2)$ and its role in mechanics and control, see [11, 3, 6].

The Lie group $SE(2)$. The elements of $SE(2)$ are pairs $g := (R_\theta, \mathbf{x})$ where $R_\theta \in SO(2)$ represents the counterclockwise rotation over an angle $\theta \in \mathbb{S}^1$, and $\mathbf{x} \in \mathbb{R}^2$ represents the translation along \mathbf{x} . There is a one-to-one correspondence between elements $g = (R_\theta, \mathbf{x}) \in SE(2)$ and 3-by-3 matrices \hat{g} of the form

$$\hat{g} = \begin{pmatrix} R_\theta & \mathbf{x} \\ 0 & 1 \end{pmatrix}. \quad (1)$$

In terms of matrices, the group multiplication in $SE(2)$ is given by matrix multiplication. In components, we have that $(R_\theta, \mathbf{x}) \cdot (R_\varphi, \mathbf{y}) = (R_{\theta+\varphi}, R_\theta \mathbf{x} + \mathbf{y})$ and $(R_\theta, \mathbf{x})^{-1} = (R_{-\theta}, -R_{-\theta} \mathbf{x})$.

The Lie algebra $\mathfrak{se}(2)$. The Lie algebra of $SE(2)$ will be denoted by $\mathfrak{se}(2)$. The elements of the 3-dimensional Lie algebra $\mathfrak{se}(2)$ can be viewed as infinitesimal rotations and translations in the plane, and are represented as vectors

$$\xi = \begin{pmatrix} \omega \\ \mathbf{v} \end{pmatrix} \in \mathbb{R}^3,$$

where $\omega \in \mathbb{R}$ and $\mathbf{v} \in \mathbb{R}^2$. There is a one-to-one correspondence between the elements ξ of $\mathfrak{se}(2)$ and 3-by-3 matrices $\hat{\xi}$ of the form

$$\hat{\xi} = \begin{pmatrix} -\omega J & \mathbf{v} \\ 0 & 0 \end{pmatrix}, \quad \text{where } J = \begin{pmatrix} 0 & 1 \\ -1 & 0 \end{pmatrix}. \quad (2)$$

In terms of matrices, the Lie bracket on $\mathfrak{se}(2)$ is given by the matrix commutator: $[\hat{\xi}, \hat{\eta}] = \hat{\xi}\hat{\eta} - \hat{\eta}\hat{\xi}$, for all $\hat{\xi}, \hat{\eta} \in \mathfrak{se}(2)$. In components, we have that $[(\omega, \mathbf{v}), (\eta, \mathbf{w})] = (0, -\omega J\mathbf{w} + \eta J\mathbf{v})$.

The elements of the dual space $\mathfrak{se}(2)^*$ are likewise column vectors in \mathbb{R}^3 , denoted as

$$\mu = \begin{pmatrix} \pi \\ \mathbf{p} \end{pmatrix},$$

with $\pi \in \mathbb{R}$ and $\mathbf{p} \in \mathbb{R}^2$. The duality pairing is given in terms of the Euclidean inner product on \mathbb{R}^3 by

$$\langle \mu, \xi \rangle := \mu^T \xi = \pi\omega + \mathbf{p}^T \mathbf{v}. \quad (3)$$

Choice of a norm on $SE(2)$. Let $m > 0$ be a fixed parameter. We define a norm on the vector space $\mathfrak{se}(2)$ by

$$\|\xi\|_{\mathfrak{se}(2)}^2 = \|(\omega, \mathbf{v})\|_{\mathfrak{se}(2)}^2 := m\omega^2 + \mathbf{v}^T \mathbf{v}, \quad (4)$$

for $\xi = (\omega, \mathbf{v}) \in \mathfrak{se}(2)$.

We extend this norm by left translation to a norm on the tangent vectors to the group $SE(2)$, given by

$$\|v_g\|_{SE(2)} = \|g^{-1}v_g\|_{\mathfrak{se}(2)} \quad (5)$$

for all $v_g \in T_g SE(2)$. Here we represent g in the matrix form (1) and the tangent vectors v_g as 3-by-3 matrices

$$v_g = \begin{pmatrix} -R_\theta J\theta' & \mathbf{x}' \\ 0 & 0 \end{pmatrix},$$

where $(\theta', \mathbf{x}') \in \mathbb{R} \times \mathbb{R}^2$. The multiplication on the right-hand side of (5) is matrix multiplication, and $g^{-1}v_g \in \mathfrak{se}(2)$. Upon expanding the matrix product, we find for the norm

$$\|v_g\|_{SE(2)}^2 = m(\theta')^2 + \|\mathbf{x}'\|^2. \quad (6)$$

Note that the norm is by definition invariant with respect to the left action of $SE(2)$ on itself:

$$\|hv_g\|_{SE(2)} = \|(hg)^{-1}hv_g\|_{\mathfrak{se}(2)} = \|g^{-1}gv_g\|_{\mathfrak{se}(2)} = \|v_g\|_{SE(2)}.$$

From now on, we will drop the subscripts on the norms just defined, and we will denote both by $\|\cdot\|$.

The action of $SE(2)$ on \mathbb{R}^2 . The group $SE(2)$ acts on the plane \mathbb{R}^2 in the standard way: an element $(R_\theta, \mathbf{x}) \in SE(2)$ transforms a point $\mathbf{c} \in \mathbb{R}^2$ into $\mathbf{c}' = R_\theta \mathbf{c} + \mathbf{x}$. This action translates into an infinitesimal action of $\mathfrak{se}(2)$ on \mathbb{R}^2 defined by $(\omega, \mathbf{v}) \cdot \mathbf{c} = -\omega J\mathbf{c} + \mathbf{v}$. For $\mathbf{c} \in \mathbb{R}^2$ fixed, we denote by $\mathfrak{se}(2)_{\mathbf{c}}$ the *isotropy subalgebra* of elements in $\mathfrak{se}(2)$ that fix \mathbf{c} , that is,

$$\mathfrak{se}(2)_{\mathbf{c}} = \{(\omega, \mathbf{v}) \in \mathfrak{se}(2) : \mathbf{v} = \omega J\mathbf{c}\}.$$

We let $\mathfrak{se}(2)_{\mathbf{c}}^\circ$ be the annihilator of $\mathfrak{se}(2)_{\mathbf{c}}$ in $\mathfrak{se}(2)^*$. In other words, $\mathfrak{se}(2)_{\mathbf{c}}^\circ$ consists of all covectors (π, \mathbf{p}) which vanish when contracted with the elements of $\mathfrak{se}(2)_{\mathbf{c}}$. A small calculation shows that

$$\mathfrak{se}(2)_{\mathbf{c}}^\circ = \{(\pi, \mathbf{p}) \in \mathfrak{se}(2)^* : \pi = -\mathbf{p} \cdot J\mathbf{c}\} \quad (7)$$

Note that $\mathfrak{se}(2)_{\mathbf{c}}$ is isomorphic to $\mathfrak{so}(2)$, while $\mathfrak{se}(2)_{\mathbf{c}}^\circ$ is isomorphic to \mathbb{R}^2 .

Lastly, we define the projection $\mathbb{P}_{\mathbf{c}} : \mathfrak{se}(2)^* \rightarrow \mathbb{R}$ by

$$\mathbb{P}_{\mathbf{c}}(\pi, \mathbf{p}) = \pi + \mathbf{p} \cdot J\mathbf{c}, \quad (8)$$

so that $\mathfrak{se}(2)_{\mathbf{c}}^\circ$ is precisely the kernel of $\mathbb{P}_{\mathbf{c}}$. This map will be useful later on.

3 Continuous Relative Geodesics in $SE(2)$

Throughout this section, we let $\mathbf{c}_0, \mathbf{c}_1 : [0, 1] \rightarrow \mathbb{R}^2$ be two fixed parametrized curves. We say that a curve $g : [0, 1] \rightarrow SE(2)$ is *admissible* with respect to \mathbf{c}_0 and \mathbf{c}_1 if

$$g(s) \cdot \mathbf{c}_0(s) = \mathbf{c}_1(s), \quad \text{for all } s \in [0, 1],$$

where the dot on the left hand side represents the standard action of $SE(2)$ on \mathbb{R}^2 . In other words, a curve $g(s) = (R_{\theta(s)}, \mathbf{x}(s))$ is admissible if

$$R_{\theta(s)}\mathbf{c}_0(s) + \mathbf{x}(s) = \mathbf{c}_1(s), \quad \text{for all } s \in [0, 1]. \quad (9)$$

3.1 The Deformation Energy

We now wish to find the admissible curves in $SE(2)$ which minimize the *deformation energy*

$$E_0 = \frac{1}{2} \int_0^1 \|g'(s)\|^2 ds, \quad (10)$$

where the norm $\|\cdot\|$ was given in (5), and the prime ' represents the derivative with respect to the curve parameter s . The deformation energy measures the change in $g(s)$ as s varies.

Definition 3.1. Let $\mathbf{c}_0, \mathbf{c}_1 : [0, 1] \rightarrow \mathbb{R}^2$ be two parametrized curves. A admissible curve $g : [0, 1] \rightarrow SE(2)$ with respect to $\mathbf{c}_0, \mathbf{c}_1$ is a relative geodesic if is a minimum of the deformation energy E_0 over all admissible curves.

Since the norm (5) is invariant with respect to the multiplication from the left by elements of $SE(2)$, we may write the deformation energy equivalently as

$$\begin{aligned} E_0 &= \frac{1}{2} \int_0^1 \|g^{-1}(s)g'(s)\|^2 ds \\ &= \frac{1}{2} \int_0^1 m\omega(s)^2 + \|\mathbf{v}(s)\|^2 ds, \end{aligned} \quad (11)$$

where in the second expression the definition (4) has been used. Here, $(\omega(s), \mathbf{v}(s)) \in \mathfrak{se}(2)$ in the Lie algebra is related to the group element $g(s) = (R_{\theta(s)}, \mathbf{x}(s))$ by means of the equations

$$\omega = \theta' \quad \text{and} \quad \mathbf{v} = R_{-\theta}\mathbf{x}', \quad (12)$$

which follow from expanding the left-trivialized derivative $g^{-1}(s)g'(s)$:

$$g^{-1}(s)g'(s) = \begin{pmatrix} R_{-\theta} & -R_{-\theta}\mathbf{x} \\ 0 & 1 \end{pmatrix} \begin{pmatrix} -R_{\theta}J\theta' & \mathbf{x}' \\ 0 & 0 \end{pmatrix} = \begin{pmatrix} -J\theta' & R_{-\theta}\mathbf{x}' \\ 0 & 0 \end{pmatrix}.$$

Using the identification (2), we then arrive at the equations (12). These relations are referred to as the *reconstruction relations*: given $\omega(s)$ and $\mathbf{v}(s)$, (12) may be viewed as a set of first-order ODEs specifying the components of $g(s)$.

For the purpose of deriving the equations that determine the extremals of E_0 , it will be convenient to add the reconstruction relations as constraints to the deformation energy, so that we obtain

$$E = \int_0^1 \frac{1}{2} \left(m\omega^2(s) + \|\mathbf{v}(s)\|^2 \right) + \pi(s)(\theta'(s) - \omega(s)) + \mathbf{p}(s)^T (R_{-\theta(s)}\mathbf{x}'(s) - \mathbf{v}(s)) ds. \quad (13)$$

Here, E depends now on the curve (R_{θ}, \mathbf{x}) , the Lie algebra elements $(\omega, \mathbf{v}) \in \mathfrak{se}(2)$, and the Lagrange multipliers (π, \mathbf{p}) , which can be viewed as elements of the dual $\mathfrak{se}(2)^*$ of the Lie algebra. It will be shown below that the critical points of this augmented functional coincide with the critical points of the original deformation energy, given in (10).

Note that E can be written in a more concise, Lie-algebraic way as

$$E = \int_0^1 \frac{1}{2} \langle\langle \xi(s), \xi(s) \rangle\rangle + \langle \mu(s), g^{-1}(s)g'(s) - \xi(s) \rangle ds, \quad (14)$$

where $\xi(s) = (\omega(s), \mathbf{v}(s)) \in \mathfrak{se}(2)$, $\mu(s) = (\pi(s), \mathbf{p}(s)) \in \mathfrak{se}(2)^*$, and the brackets $\langle\langle \cdot, \cdot \rangle\rangle$ refer to the inner product associated to the norm (4). This energy function can be generalized in a straightforward way to the case of relative geodesics with values in an arbitrary Lie group G .

The variational principle for (14), in which the configuration variables, velocities and momenta are varied independently while the reconstruction equations are treated as constraints, is a particular example of the *Hamiltonian-Pontryagin principle* (see [16]). A version of the Hamilton-Pontryagin principle specific to Lie groups can be found in [2]; see also [1]. Our variational principle is also related to the *Clebsch variational principle* of [4, 5], although it does not coincide with it.

3.2 The Continuous Equations of Motion

We now derive the differential equations that describe the critical points of the deformation energy. Because of the analogy with the Euler-Lagrange equations in mechanics, we will refer to these equations as equations of motion.

We take variations of the augmented deformation energy E in (13) with respect to the variables $(\theta, \mathbf{x}, \omega, \mathbf{v}, \pi, \mathbf{p})$, where the velocities (ω, \mathbf{v}) and the momenta (π, \mathbf{p}) are varied freely, while the configuration variables (θ, \mathbf{x}) are varied with respect to variations that preserve the admissibility constraint (9). On the level of the variations, the infinitesimal version of this constraint is given by

$$-R_\theta J \mathbf{c}_0 \delta\theta + \delta\mathbf{x} = 0, \quad (15)$$

where the matrix J was given in (2), and this relation allows us to eliminate the variation $\delta\mathbf{x}$ in terms of $\delta\theta$. This infinitesimal constraint was obtained by taking a one-parameter family $(\theta_\epsilon(s), \mathbf{x}_\epsilon(s))$ of admissible curves in $SE(2)$: taking the derivative of the admissibility constraint (9) with respect to ϵ , and putting

$$\delta\theta = \left. \frac{d\theta_\epsilon}{d\epsilon} \right|_{\epsilon=0} \quad \text{and} \quad \delta\mathbf{x} = \left. \frac{d\mathbf{x}_\epsilon}{d\epsilon} \right|_{\epsilon=0}$$

then gives (15).

Taking variations of E first with respect to π and \mathbf{p} results in

$$DE \cdot \delta\pi = \int_0^1 \delta\pi(s)(\theta'(s) - \omega(s)) ds$$

and

$$DE \cdot \delta\mathbf{p} = \int_0^1 \delta\mathbf{p}(s)^T (R_{-\theta(s)} \mathbf{x}'(s) - \mathbf{v}(s)) ds,$$

so that if a curve $s \mapsto (\theta(s), \mathbf{x}(s), \omega(s), \mathbf{v}(s), \pi, \mathbf{p}(s))$ is a critical point of E then the reconstruction equations (12) must hold. Taking variations with respect to the velocities ω and \mathbf{v} similarly results in

$$DE \cdot \delta\omega = \int_0^1 (m\omega(s) - \pi(s)) \delta\omega(s) ds$$

and

$$DE \cdot \delta\mathbf{v} = \int_0^1 (\mathbf{v}(s) - \mathbf{p}(s)) \cdot \mathbf{v}(s) ds,$$

so that for a critical point of E the following Legendre transformations between the velocities and the momenta must hold:

$$\mathbf{p} = \mathbf{v} \quad \text{and} \quad \pi = m\omega. \quad (16)$$

Lastly, taking variations with respect to the configuration variables (θ, \mathbf{x}) we obtain

$$\begin{aligned} \delta E = \int_0^1 \left[\left(-\frac{d\pi}{ds} + \mathbf{p}^T R_{-\theta} J \mathbf{x}' \right) \delta\theta - \frac{d}{ds} (R_{\theta} \mathbf{p})^T \delta \mathbf{x} \right] ds \\ + \left(\pi \delta\theta + (R_{\theta} \mathbf{p})^T \delta \mathbf{x} \right) \Big|_{s=0,1}, \end{aligned}$$

where we have integrated by parts. We now use (15) to eliminate $\delta \mathbf{x}$ in function of $\delta\theta$, and we obtain

$$\begin{aligned} \delta E = \int_0^1 \left(-\frac{d\pi}{ds} + \mathbf{p}^T R_{-\theta} J \mathbf{x}' - \frac{d}{ds} (R_{\theta} \mathbf{p})^T R_{\theta} J \mathbf{c}_0 \right) \delta\theta ds \\ + \left(\pi + \mathbf{p}^T J \mathbf{c}_0 \right) \delta\theta \Big|_{s=0,1}. \end{aligned}$$

Since $\delta\theta$ is arbitrary, we see that δE vanishes whenever the expressions preceding $\delta\theta$ on the right-hand side vanish, so that

$$-\frac{d\pi}{ds} + \mathbf{p}^T R_{-\theta} J \mathbf{x}' - \frac{d}{ds} (R_{\theta} \mathbf{p})^T R_{\theta} J \mathbf{c}_0 = 0, \quad (17)$$

with boundary conditions

$$\pi + \mathbf{p}^T J \mathbf{c}_0 = 0 \quad \text{for } s = 0, 1.$$

Note that in these equations, θ and \mathbf{x} are not arbitrary, but are related by the admissibility constraint (9). By writing (17) in terms of the Lie algebra quantities (ω, \mathbf{v}) , and with some simple algebraic simplifications, we finally arrive at the following result.

Theorem 3.2. *Let $\mathbf{c}_0, \mathbf{c}_1 : [0, 1] \rightarrow \mathbb{R}^2$ be two parametrized curves. An admissible curve $(R_{\theta(s)}, \mathbf{x}(s))$ in $SE(2)$ is a critical point of the deformation energy E if and only if the following scalar equation holds:*

$$m\omega' - \mathbf{c}_0^T J \mathbf{v}' - \mathbf{c}_0^T \mathbf{v} \theta' = 0, \quad (18)$$

with natural boundary conditions $m\omega + \mathbf{v}^T J \mathbf{c}_0 = 0$ for $s = 0, 1$. Here, ω and \mathbf{v} are given in terms of θ and \mathbf{x} by the reconstruction relations (12), and the admissibility constraint (9) holds.

As the relative geodesics are precisely the minima of the deformation energy E , restricted to the space of admissible curves, the equation (18) is a necessary condition for a curve $g : [0, 1] \rightarrow SE(2)$ to be a relative geodesic.

The equation of motion (18) can be written in a form which involves the angle θ only. To this end, we differentiate the admissibility constraint (9) with respect to s and multiply from the left by $R_{-\theta}$ to obtain

$$\mathbf{v} = R_{-\theta} \mathbf{c}'_1 - \mathbf{c}'_0 + J \mathbf{c}_0 \theta'.$$

One further differentiation leads to

$$\mathbf{v}' = R_{-\theta} J \mathbf{c}'_1 \theta' + R_{-\theta} \mathbf{c}''_1 - \mathbf{c}''_0 + J \mathbf{c}'_0 \theta' + J \mathbf{c}_0 \theta''.$$

Substituting these two relations into (18) leads after some simplifications to the following non-autonomous second-order ODE for θ :

$$(m + \|\mathbf{c}_0\|^2)\theta'' + 2\mathbf{c}_0^T \mathbf{c}'_0 \theta' + \mathbf{c}_0^T J(\mathbf{c}_0'' - R_{-\theta} \mathbf{c}_1'') = 0,$$

with boundary conditions

$$(m + \|\mathbf{c}_0\|^2)\theta' + \mathbf{c}_0^T J(\mathbf{c}'_0 - R_{-\theta} \mathbf{c}'_1) = 0 \quad \text{for } s = 0, 1.$$

Given the two curves \mathbf{c}_0 and \mathbf{c}_1 , the previous equations form a boundary-value problem for θ . Once θ is determined from these equations, the linear displacement \mathbf{x} can be found from the admissibility constraint (9).

A direct derivation of the equations of motion. In this section we present an alternative derivation of the equations (18), which does not use the Euler-Poincaré framework. This derivation is arguably somewhat more straightforward than the one presented earlier, and we will use the resulting Euler-Lagrange equations extensively in Section 3.3 below. The advantage of the Euler-Poincaré equations, however, is that they can easily be discretized, as we shall show in Section 4.

We begin by introducing the function \mathcal{E}_0 given by

$$\mathcal{E}_0 = \frac{m}{2}(\theta')^2 + \frac{1}{2} \|\mathbf{x}'\|^2.$$

Note that \mathcal{E}_0 is precisely the integrand of the deformation energy E_0 in (11). We now take the derivative of the admissibility constraint (9), and use the resulting equation to obtain an expression for \mathbf{x}' . Upon substituting this expression into \mathcal{E}_0 , we obtain a function ℓ which depends on θ and θ' , and is given by

$$\ell = \frac{m}{2}(\theta')^2 + \frac{1}{2} \|R_{-\theta} \mathbf{c}'_1 - \mathbf{c}'_0 + J\mathbf{c}_0 \theta'\|^2. \quad (19)$$

The function ℓ can now be viewed as a Lagrangian function on the tangent bundle TS^1 ; its Euler-Lagrange equations are

$$\frac{d}{ds} \left(\frac{\partial \ell}{\partial \theta'} \right) - \frac{\partial \ell}{\partial \theta} = 0 \quad (20)$$

with natural boundary conditions

$$\frac{\partial \ell}{\partial \theta'} = 0, \quad \text{for } s = 0, 1.$$

For further reference, we define the momentum conjugate to θ as

$$p := \frac{\partial \ell}{\partial \theta'} = (m + \|\mathbf{c}_0\|^2)\theta' + (\mathbf{c}'_1)^T R_{\theta} J \mathbf{c}_0 - (\mathbf{c}'_0)^T J \mathbf{c}_0, \quad (21)$$

and compute

$$\frac{\partial \ell}{\partial \theta} = (\mathbf{c}_0)^T R_{-\theta} \mathbf{c}'_1 \theta' - (\mathbf{c}'_0)^T R_{-\theta} J \mathbf{c}'_1.$$

By substituting these expressions into the Euler-Lagrange equations (20), we obtain yet another set of equations characterizing relative geodesics, which we summarize in the following theorem.

Theorem 3.3. *Let $\mathbf{c}_0, \mathbf{c}_1 : [0, 1] \rightarrow \mathbb{R}^2$ be two parametrized curves. An admissible curve $(R_{\theta(s)}, \mathbf{x}(s))$ in $SE(2)$ is a critical point of the deformation energy E_0 if and only if the following Euler-Lagrange equation for θ holds:*

$$\frac{dp}{ds} = (\mathbf{c}_0)^T R_{-\theta} \mathbf{c}'_1 \theta' - (\mathbf{c}'_0)^T R_{-\theta} J \mathbf{c}'_1, \quad (22)$$

with natural boundary conditions given by $p = 0$ for $s = 0, 1$. Here $p(s)$ is given by (21) and $\mathbf{x}(s)$ is expressed as a function of $\theta(s)$ using the admissibility constraint (9).

The procedure of substituting the constraints into the deformation energy to obtain a Lagrangian function which depends on fewer degrees of freedom is similar to the approach of Chaplygin for systems with nonholonomic kinematic constraints (see [10] and the references therein). In this approach, one eliminates the constrained degrees of freedom to obtain a system of reduced Euler-Lagrange equations with gyroscopic forces. The latter vanish if the constraints are integrable, as is the case for relative geodesics.

3.3 Discrepancy between Planar Curves

Definition 3.4. *Let $\mathbf{c}_0, \mathbf{c}_1 : [0, 1] \rightarrow \mathbb{R}^2$ be two parametrized curves in the plane. The discrepancy $\delta(\mathbf{c}_0, \mathbf{c}_1)$ between \mathbf{c}_0 and \mathbf{c}_1 is the minimum of the deformation energy E_0 over all $(\mathbf{c}_0, \mathbf{c}_1)$ -admissible curves:*

$$\delta(\mathbf{c}_0, \mathbf{c}_1) = \min_{g(\cdot) \in \text{Adm}(\mathbf{c}_0, \mathbf{c}_1)} E_0(g'),$$

where $\text{Adm}(\mathbf{c}_0, \mathbf{c}_1)$ is the set of all $(\mathbf{c}_0, \mathbf{c}_1)$ -admissible curves.

Note that the admissible curve $g : [0, 1] \rightarrow SE(2)$ which minimizes E_0 can be found among the solutions of the equations of motion derived in the previous section.

Asymmetry of the discrepancy. The discrepancy $\delta(\mathbf{c}_0, \mathbf{c}_1)$ provides a measure of the difference between the curves \mathbf{c}_0 and \mathbf{c}_1 . In this section, we show that the discrepancy is in general not symmetric, that is, $\delta(\mathbf{c}_0, \mathbf{c}_1)$ differs in general from $\delta(\mathbf{c}_1, \mathbf{c}_0)$.

Throughout the remainder of this section, we use the formulation of the Euler-Lagrange equations given in Theorem 3.3.

Lemma 3.5. *Let $\mathbf{c}_0(s) = \mathbf{0}$ for all s . The geodesics relative to $(\mathbf{c}_0, \mathbf{c}_1)$ are parametrized by $\theta(0)$, and in each case*

$$\delta(\mathbf{c}_0, \mathbf{c}_1) = \frac{1}{2} \int_0^1 \|\mathbf{c}'_1\|^2 ds.$$

Proof. For a geodesic relative to $(\mathbf{c}_0, \mathbf{c}_1)$ we have that $p = m\theta'$, and from the Euler-Lagrange equations (22) it follows that $m\theta'' = 0$, so that θ is an affine function of s . By using the natural boundary conditions, it follows that θ is constant. Conversely any constant θ satisfies the Euler-Lagrange equations (22) and the natural boundary conditions, and therefore defines a relative geodesic. \square

Lemma 3.6. *Let $\mathbf{c}_1(s) = \mathbf{0}$ for all s . The geodesics relative to $(\mathbf{c}_0, \mathbf{c}_1)$ are parametrized by $\theta(0)$, and in each case the discrepancy is given by*

$$\delta(\mathbf{c}_0, \mathbf{c}_1) = \frac{1}{2} \int_0^1 \left(\|\mathbf{c}'_0\|^2 - \frac{((\mathbf{c}'_0)^T J \mathbf{c}_0)^2}{m + \|\mathbf{c}_0\|^2} \right) ds. \quad (23)$$

Proof. By (22), p is constant, and by the natural boundary conditions, p is identically 0, so that

$$\theta' = \frac{(\mathbf{c}'_0)^T J \mathbf{c}_0}{m + \|\mathbf{c}_0\|^2}.$$

By substituting this expression for θ' into the deformation energy, we obtain (23) after some simplifications. \square

Proposition 3.7. *Let $\mathbf{c}_0(s) = \mathbf{0}$ for all s . Then $\delta(\mathbf{c}_1, \mathbf{c}_0) \leq \delta(\mathbf{c}_0, \mathbf{c}_1)$, with equality only in the case where, for some $\mathbf{x}_0 \in \mathbb{R}^2$ and some $\phi : [0, 1] \rightarrow \mathbb{R}$, $\mathbf{c}_1(s) = \phi(s)\mathbf{x}_0$.*

Proof. Combining lemmas 3.5 and 3.6, we have that

$$\delta(\mathbf{c}_1, \mathbf{c}_0) = \delta(\mathbf{c}_0, \mathbf{c}_1) - \int_0^1 \frac{((\mathbf{c}'_1)^T J \mathbf{c}_1)^2}{m + \|\mathbf{c}_1\|^2} ds,$$

so that $\delta(\mathbf{c}_1, \mathbf{c}_0) < \delta(\mathbf{c}_0, \mathbf{c}_1)$ except when $(\mathbf{c}'_1)^T J \mathbf{c}_1$ vanishes identically. In this case, $\mathbf{c}'_1(s) = \mu(s)\mathbf{c}_1(s)$ for some function μ , and therefore $\mathbf{c}_1(s) = \phi(s)\mathbf{x}_0$, with $\phi(s) = e^{\mu(s)}$. \square

As an illustration, we take $\mathbf{c}_0(s) = \mathbf{0}$ and $\mathbf{c}_1(s) = (\cos(\pi s), \sin(\pi s))$ for $s \in [0, 1]$. By Lemmas 3.5 and 3.6, we have that

$$\delta(\mathbf{c}_0, \mathbf{c}_1) = \frac{\pi^2}{2} \approx 4.93, \quad \text{and} \quad \delta(\mathbf{c}_1, \mathbf{c}_0) = \frac{1}{2} \frac{m}{m+1} \pi^2,$$

so that indeed $\delta(\mathbf{c}_0, \mathbf{c}_1) > \delta(\mathbf{c}_1, \mathbf{c}_0)$.

Non-minimising relative geodesics. There are always at least two geodesics relative to $(\mathbf{c}_0, \mathbf{c}_1)$, corresponding to critical points of the deformation energy E_0 regarded as a function of θ_0 where the relative geodesic $s \mapsto (R_{\theta(s)}, \mathbf{x}(s))$ satisfies (22) for all s and the natural boundary conditions at $s = 0$.

Proposition 3.8. *Let \mathbf{c}_1 be a nonconstant affine line segment, and suppose $\mathbf{c}_0(0) = \mathbf{0}$ with $\mathbf{c}_0(1) \neq \mathbf{0}$. Then there are exactly two geodesics relative to $(\mathbf{c}_0, \mathbf{c}_1)$, and these are determined by*

$$\theta(s) = \int_s^1 \frac{(\mathbf{c}'_0(u))^T J \mathbf{c}_0(u)}{m + \|\mathbf{c}_0(u)\|^2} du \pm \chi_1$$

with χ_1 the angle between $\mathbf{c}_0(1)$ and $\mathbf{c}'_1(1)$. Only one of these relative geodesics is a global minimiser of E_0 .

Proof. Since $\mathbf{c}'_1(s) =: \mathbf{C}$, where \mathbf{C} is a constant vector, the right-hand side of the Euler-Lagrange equations (22) can be written as a total s -derivative:

$$(\mathbf{c}_0)^T R_{-\theta} \mathbf{c}'_1 \theta' - (\mathbf{c}'_0)^T R_{-\theta} J \mathbf{c}'_1 = -\frac{d}{ds} (\mathbf{c}'_0)^T R_{-\theta} J \mathbf{C}.$$

Consequently, the Euler-Lagrange equations imply that the quantity

$$\hat{p} := p + \mathbf{c}'_0{}^T R_{-\theta} J \mathbf{C} = (m + \|\mathbf{c}_0\|^2) \theta' - (\mathbf{c}'_0)^T J \mathbf{c}_0 \quad (24)$$

is conserved. Since $\mathbf{c}_0(0) = \mathbf{0}$ and $p = 0$ at $s = 0$, $\hat{p}(s)$ is identically 0. So, for some θ_0 ,

$$\theta(s) = \theta_0 - \int_0^s \frac{(\mathbf{c}'_0(u))^T J \mathbf{c}_0(u)}{m + \|\mathbf{c}_0(u)\|^2} du.$$

At the terminal end of the curve, i.e. for $s = 1$, we have that $p(1) = \hat{p}(1) = 0$. From (21) it then follows that $p(1) - \hat{p}(1) = \mathbf{C}^T R_{\theta(1)} J \mathbf{c}_0(1) = 0$, namely $R_{\theta(1)} \mathbf{c}_0(1)$ is a multiple of \mathbf{C} , so that $\theta(1) = \pm \chi_1$ for some angle χ_1 . As a consequence, the initial angle θ_0 satisfies

$$\theta_0 = \int_0^1 \frac{(\mathbf{c}'_0(u))^T J \mathbf{c}_0(u)}{m + \|\mathbf{c}_0(u)\|^2} du \pm \chi_1.$$

Considering E_0 as a function of $e^{i\theta_0} \in \mathbb{S}^1$, one of these values of θ_0 is a point of global maximum, the other is a point of global minimum, and E_0 has no other critical points. \square

As an illustration, we consider the discrepancy between two line segments. We take $\mathbf{c}_0(s) = s\mathbf{e}_x$ and $\mathbf{c}_1(s) = s\mathbf{e}_y$, with $\mathbf{e}_x, \mathbf{e}_y$ the standard unit vectors along the positive x - and y -axis, respectively. From the previous proposition, we deduce that $\theta(s) = \pm\pi/2$ for all s .

For the solution with $\theta(s) = \pi/2$, the admissibility condition results in $\mathbf{x}(s) = \mathbf{0}$ for all s . In this case, the effect of applying the relative geodesic is to rotate all of the points of \mathbf{c}_0 over $\pi/2$, and not effect any translation. As the relative geodesic is constant, $g(s) = (R_{\pi/2}, \mathbf{0})$, the deformation energy vanishes identically, so that $g(s)$ is a minimizing geodesic. In the case where $\theta(s) = -\pi/2$, the admissibility constraint yields $\mathbf{x}(s) = 2s\mathbf{e}_y$ so that the effect of the relative geodesic is to rotate each point $\mathbf{c}_0(s)$ over $-\pi/2$, followed by a translation over $2s\mathbf{e}_y$. The deformation energy in this case is $E = 2$.

Remark 3.9. In the proof of Proposition 3.8, we have seen that the quantity \hat{p} is conserved when $\mathbf{c}'_1(s) = \mathbf{C}$ with \mathbf{C} constant. A natural question to ask is the following: Is there a continuous symmetry whose associated conserved quantity (through Noether's theorem) is precisely \hat{p} ? To see that this is indeed the case, we return to the Lagrangian ℓ in (19) which we rewrite as

$$\begin{aligned} \ell &= \frac{m}{2} (\theta')^2 + \frac{1}{2} \left(\|\mathbf{c}'_1\|^2 + \|\mathbf{c}'_0 - J \mathbf{c}_0 \theta'\|^2 \right) + (\mathbf{c}'_1)^T R_\theta (J \mathbf{c}_0 \theta' - \mathbf{c}'_0) \\ &= \hat{\ell} - \frac{d}{ds} \left((\mathbf{c}'_1)^T R_\theta \mathbf{c}_0 \right), \end{aligned}$$

where $\hat{\ell}$ is defined as

$$\hat{\ell} = \frac{m}{2} (\theta')^2 + \frac{1}{2} \left(\|\mathbf{c}'_1\|^2 + \|\mathbf{c}'_0 - J \mathbf{c}_0 \theta'\|^2 \right) + (\mathbf{c}'_1)^T R_\theta \mathbf{c}_0. \quad (25)$$

Since ℓ and $\hat{\ell}$ differ by a total s -derivative, they give rise to the same Euler-Lagrange equations (see [13]). For $\hat{\ell}$, the momentum conjugate to θ is precisely the quantity \hat{p} defined in (24):

$$\hat{p} = \frac{\partial \hat{\ell}}{\partial \theta'} = (m + \|\mathbf{c}_0\|^2)\theta' - (\mathbf{c}'_0)^T J \mathbf{c}_0.$$

In the case that $\mathbf{c}''_1 = 0$, we see from (25) that $\hat{\ell}$ does not depend on θ , so that \hat{p} is a conserved quantity:

$$\frac{d\hat{p}}{ds} = \frac{\partial \hat{\ell}}{\partial \theta} = 0 \quad (\text{when } \mathbf{c}''_1 = 0).$$

4 Discrete Relative Geodesics in $SE(2)$

We now assume we have two discrete curves $(\mathbf{c}_0)_k, (\mathbf{c}_1)_k$, $k = 0, \dots, N$ of N points each. We wish to find a discrete curve $g_k = (R_{\theta_k}, \mathbf{x}_k)$, $k = 0, \dots, N$ in $SE(2)$ which is *admissible* in the sense that

$$R_{\theta_k}(\mathbf{c}_0)_k + \mathbf{x}_k = (\mathbf{c}_1)_k \quad (26)$$

for all $k = 0, \dots, N$. To derive a discrete version of the deformation energy E , we need to discretize the spatial derivatives that appear in (14). We do this by means of the Cayley map from $\mathfrak{se}(2)$ to $SE(2)$.

Our way of discretizing the variational principle, as well as the discrete equations obtained from it, is inspired by the *discrete Hamilton-Pontryagin principle* of [1]; see also [9] and [14]. As in the continuous case, the main difficulty here is the incorporation of the admissibility constraint (26).

4.1 The Cayley Map

Definition. The Cayley map $\text{Cay} : \mathfrak{se}(2) \rightarrow SE(2)$ is given by

$$\text{Cay}(\xi) = \begin{pmatrix} \hat{R}_\omega & \hat{\mathbf{x}}_\xi \\ 0 & 1 \end{pmatrix}, \quad (27)$$

where, if $\xi = (\omega, \mathbf{v}) \in \mathfrak{se}(2)$,

$$\hat{R}_\omega := \frac{1}{1 + \omega^2/4} \begin{pmatrix} 1 - \omega^2/4 & -\omega \\ \omega & 1 - \omega^2/4 \end{pmatrix}, \quad \text{and} \quad \hat{\mathbf{x}}_\xi := \frac{1}{1 + \omega^2/4} \begin{pmatrix} v_1 - \omega v_2/2 \\ v_2 + \omega v_1/2 \end{pmatrix}, \quad (28)$$

with $\mathbf{v} = (v_1, v_2)$. Note that \hat{R}_ω depends only on ω and is in fact the Cayley transform in $SO(2)$.

The Cayley map is in fact a $(1, 1)$ -Padé approximation to the exponential map from $\mathfrak{se}(2)$. In contrast to the exponential, the Cayley map has the advantage that it is an algebraic map, so that it is easily computable.

The Cayley map shares with the exponential map a number of useful properties, which will be used in some of the derivations below:

$$D \text{Cay}(0) = \text{id.} \quad \text{and} \quad \text{Cay}(-\xi) = \text{Cay}(\xi)^{-1}, \quad (29)$$

for all $\xi \in \mathfrak{se}(2)$.

The Right-Trivialized Derivative. For our purposes, we will need the *right-trivialized derivative* of the Cayley map, defined by

$$d\text{Cay}_\xi(\eta) := (D\text{Cay}(\xi) \cdot \eta)\text{Cay}(\xi)^{-1}; \quad (30)$$

see [7]. Note that $D\text{Cay}(\xi) \cdot \eta$ is an element of $T_\xi SE(2)$, which is translated back to $\mathfrak{se}(2)$ by right-multiplication by $\text{Cay}(\xi)^{-1}$. In this way, $d\text{Cay}$ is a map from $\mathfrak{se}(2) \times \mathfrak{se}(2)$ to $\mathfrak{se}(2)$ which is linear in the second argument.

For fixed $\xi \in \mathfrak{se}(2)$, we denote the inverse of $d\text{Cay}_\xi$ by $d\text{Cay}_\xi^{-1}$. From (30), we have that

$$d\text{Cay}_\xi^{-1}(\eta) = [D\text{Cay}(\xi)]^{-1} \cdot (\eta \text{Cay}(\xi)). \quad (31)$$

For the group $SE(2)$, the Cayley map and its derivatives were computed explicitly in [8]. Keeping in mind that the elements of $\mathfrak{se}(2)$ are represented as column vectors, for each $\xi \in \mathfrak{se}(2)$, $d\text{Cay}_\xi^{-1}$ is a linear transformation from $\mathfrak{se}(2)$ to itself, given by

$$d\text{Cay}_\xi^{-1}(\eta) = M(\xi)\eta$$

where, for $\xi = (\omega, v, w)$, the matrix $M(\xi)$ is given by

$$M(\xi) = \begin{pmatrix} 1 + \omega^2/4 & 0 & 0 \\ -w/2 + \omega v/4 & 1 & \omega/2 \\ v/2 + \omega w/4 & -\omega/2 & 1 \end{pmatrix}. \quad (32)$$

For future reference, we record the following property of the right-trivialized derivative (see [1]): for all $\xi, \eta \in \mathfrak{se}(2)$

$$d\text{Cay}_\xi^{-1}(\eta) = d\text{Cay}_{-\xi}^{-1}(\text{Ad}_{\text{Cay}(-\xi)}\eta), \quad (33)$$

where Ad is the adjoint action of $SE(2)$ on $\mathfrak{se}(2)$, defined by $\text{Ad}_g(\xi) = g\xi g^{-1}$, where the elements on the right-hand side are interpreted as matrices, as in (1) and (2).

Lastly, for each $\xi \in \mathfrak{se}(2)$, its adjoint, $(d\text{Cay}_\xi^{-1})^*$, is a linear map from $\mathfrak{se}(2)^*$ to itself, defined by

$$\langle (d\text{Cay}_\xi^{-1})^*\mu, \eta \rangle = \langle \mu, d\text{Cay}_\xi^{-1}(\eta) \rangle, \quad (34)$$

relative to the duality pairing (3). Explicitly,

$$(d\text{Cay}_\xi^{-1})^*\mu = M(\xi)^T\mu. \quad (35)$$

We will use the Cayley map to provide a parametrization of a neighborhood of the identity in $SE(2)$ by means of the Lie algebra $\mathfrak{se}(2)$, but it is possible to replace the Cayley map by any other local diffeomorphism satisfying (29) from $\mathfrak{se}(2)$ to $SE(2)$, such as the exponential map. The Cayley map, however, has the advantage that it is efficiently computable, and its derivative is particularly easy to characterize.

4.2 The Deformation Energy

The Discrete Reconstruction Relations. Using the Cayley map, we discretize the reconstruction relations (12) as follows. Given two successive elements g_k, g_{k+1} in $SE(2)$, we define the *update element* $\xi_k \in \mathfrak{se}(2)$ by

$$\text{Cay}(h\xi_k) = g_k^{-1}g_{k+1}. \quad (36)$$

This is the discrete counterpart of the relation $\xi = g^{-1}g'$. Explicitly, if $\xi_k = (\omega_k, \mathbf{v}_k)$ and $g_i = (R_{\theta_i}, \mathbf{x}_i)$, $i = k, k+1$, we have for the components

$$\hat{R}_{h\omega_k} = R_{\theta_{k+1}-\theta_k}, \quad \text{and} \quad \hat{\mathbf{x}}_{h\xi_k} = R_{-\theta_k}(\mathbf{x}_{k+1} - \mathbf{x}_k). \quad (37)$$

The first relation is equivalent to the following trigonometric relation:

$$\frac{h\omega_k}{2} = \tan\left(\frac{\theta_{k+1} - \theta_k}{2}\right). \quad (38)$$

The Deformation Energy. To discretize the deformation energy, we now proceed as in the continuous case. We define E as

$$E = h \sum_{k=0}^{N-1} \left(\frac{1}{2} \langle \xi_k, \xi_k \rangle + \left\langle \mu_k, \frac{1}{h} \text{Cay}^{-1}(g_k^{-1}g_{k+1}) - \xi_k \right\rangle \right), \quad (39)$$

which can be viewed as the discrete counterpart of (14). Here, $g_k \in SE(2)$, $\xi_k \in \mathfrak{se}(2)$ and $\mu_k \in \mathfrak{se}(2)^*$ are independent variables. As mentioned at the beginning of this section, this energy function was originally introduced in [1], and the derivations up to (42), when we have to enforce the discrete admissibility constraint, will follow that paper.

By taking variations with respect to μ_k , we recover the definition (36) of the update element ξ_k . By taking variations with respect to ξ_k , we arrive at the equation $\mu_k = \xi_k^\flat$, or explicitly

$$\pi_k = m\omega_k, \quad \text{and} \quad \mathbf{p}_k = \mathbf{v}_k. \quad (40)$$

Lastly, by taking variations with respect to the group element g_k we obtain

$$\delta E = \sum_{k=0}^{N-1} \langle \mu_k, D \text{Cay}^{-1}(g_k^{-1}g_{k+1}) \cdot (-g_k^{-1}\delta g_k g_k^{-1}g_{k+1} + g_k^{-1}\delta g_{k+1}) \rangle,$$

where we have used the fact that $\delta g_k^{-1} = -g_k^{-1}\delta g_k g_k^{-1}$. We now introduce the quantity $\sigma_k := g_k^{-1}\delta g_k$ and focus first on the first derivative term, which we write as

$$D \text{Cay}^{-1}(g_k^{-1}g_{k+1}) \cdot (\sigma_k g_k^{-1}g_{k+1}) = [D \text{Cay}(h\xi_k)]^{-1} \cdot (\sigma_k \text{Cay}(h\xi_k)) = d\text{Cay}_{h\xi_k}^{-1}(\sigma_k),$$

where we have used the definition (31) of $d\text{Cay}^{-1}$, together with the expression (36) for the update element. For the second term in δE , we proceed along similar lines:

$$\begin{aligned} D \text{Cay}^{-1}(g_k^{-1}g_{k+1}) \cdot (g_k^{-1}\delta g_{k+1}) &= D \text{Cay}^{-1}(g_k^{-1}g_{k+1}) \cdot (g_k^{-1}g_{k+1}\sigma_{k+1}) \\ &= [D \text{Cay}(h\xi_k)]^{-1} \cdot (\text{Ad}_{\text{Cay}(h\xi_k)}(\sigma_{k+1}) \text{Cay}(h\xi_k)) \\ &= d\text{Cay}_{h\xi_k}^{-1}(\text{Ad}_{\text{Cay}(h\xi_k)}(\sigma_{k+1})) \\ &= d\text{Cay}_{-h\xi_k}^{-1}(\sigma_{k+1}) \end{aligned}$$

where we have used the property (33) in the last step.

Substituting both of these expressions for the derivatives back into the expression for δE , we arrive at

$$\begin{aligned}\delta E &= \sum_{k=0}^{N-1} \left\{ - \left\langle \mu_k, \text{dCay}_{h\xi_k}^{-1}(\sigma_k) \right\rangle + \left\langle \mu_k, \text{dCay}_{-h\xi_k}^{-1}(\sigma_{k+1}) \right\rangle \right\} \\ &= \sum_{k=0}^{N-1} \left\{ - \left\langle (\text{dCay}_{h\xi_k}^{-1})^* \mu_k, \sigma_k \right\rangle + \left\langle (\text{dCay}_{-h\xi_k}^{-1})^* \mu_k, \sigma_{k+1} \right\rangle \right\},\end{aligned}$$

where we have introduced the adjoint of the linear map $\text{dCay}_{h\xi_k}^{-1}$ using the definition (34). We now rearrange the terms in the sum to get

$$\begin{aligned}\delta E &= - \left\langle (\text{dCay}_{h\xi_0}^{-1})^* \mu_0, \sigma_0 \right\rangle + \left\langle (\text{dCay}_{-h\xi_{N-1}}^{-1})^* \mu_{N-1}, \sigma_N \right\rangle \\ &\quad + \sum_{k=1}^{N-1} \left\langle -(\text{dCay}_{h\xi_k}^{-1})^* \mu_k + (\text{dCay}_{-h\xi_{k-1}}^{-1})^* \mu_{k-1}, \sigma_k \right\rangle.\end{aligned}\tag{41}$$

It remains for us to obtain an expression for the variations $\sigma_k = g_k^{-1} \delta g_k$. Since E is varied over all discrete admissible curves, (26) must hold, and by differentiating and multiplying by $R_{-\theta_k}$, we find

$$-\delta\theta_k J(\mathbf{c}_0)_k + \mathbf{w}_k = 0,\tag{42}$$

where $\delta\theta_k$ and \mathbf{w}_k are the components of σ_k . Note that if $\delta g_k = (\delta\theta_k, \delta\mathbf{x}_k)$, then $\mathbf{w}_k = R_{-\theta_k} \delta\mathbf{x}_k$. In other words, σ_k is an element of $\mathfrak{se}(2)_{(\mathbf{c}_0)_k}$. Since σ_k is otherwise arbitrary, we arrive at the following weak form of the discrete equations of motion:

$$\left\langle -(\text{dCay}_{h\xi_k}^{-1})^* \mu_k + (\text{dCay}_{-h\xi_{k-1}}^{-1})^* \mu_{k-1}, \sigma_k \right\rangle = 0\tag{43}$$

for all $\sigma_k \in \mathfrak{se}(2)_{(\mathbf{c}_0)_k}$, together with the weak boundary conditions

$$\left\langle (\text{dCay}_{h\xi_0}^{-1})^* \mu_0, \sigma_0 \right\rangle = 0 \quad \text{and} \quad \left\langle (\text{dCay}_{-h\xi_{N-1}}^{-1})^* \mu_{N-1}, \sigma_N \right\rangle = 0\tag{44}$$

for all $\sigma_0 \in \mathfrak{se}(2)_{(\mathbf{c}_0)_0}$ and $\sigma_N \in \mathfrak{se}(2)_{(\mathbf{c}_0)_N}$. Another way to formulate the equations of motion is to observe that the left-most factor in each of these contractions must take values in $\mathfrak{se}(2)_{(\mathbf{c}_0)_k}^\circ$, defined in (7). In this way, we arrive at the following theorem.

Theorem 4.1. *A discrete admissible curve $g_k \in SE(2)$, $k = 0, \dots, N$, is a critical point of the deformation energy E if and only if (43) holds, with boundary conditions (44). This is equivalent to*

$$-(\text{dCay}_{h\xi_k}^{-1})^* \mu_k + (\text{dCay}_{-h\xi_{k-1}}^{-1})^* \mu_{k-1} \in \mathfrak{se}(2)_{(\mathbf{c}_0)_k}^\circ\tag{45}$$

together with the boundary conditions

$$(\text{dCay}_{h\xi_0}^{-1})^* \mu_0 \in \mathfrak{se}(2)_{(\mathbf{c}_0)_0}^\circ \quad \text{and} \quad (\text{dCay}_{-h\xi_{N-1}}^{-1})^* \mu_{N-1} \in \mathfrak{se}(2)_{(\mathbf{c}_0)_N}^\circ.$$

The Discrete Constraint. The equation (45) is a single scalar equation, which in itself is insufficient to determine all three components of $\xi_k = (\omega_k, \mathbf{v}_k)$. We now show that the admissibility condition (26) gives rise to two further equations, allowing all three components of ξ_k to be determined.

By taking the admissibility constraint for k and subtracting it from the constraint for $k + 1$, we obtain (after multiplying from the left by $R_{-\theta_k}$) that

$$R_{\theta_{k+1}-\theta_k}(\mathbf{c}_0)_{k+1} - (\mathbf{c}_0)_k + R_{-\theta_k}(\mathbf{x}_{k+1} - \mathbf{x}_k) = R_{-\theta_k}((\mathbf{c}_1)_{k+1} - (\mathbf{c}_1)_k).$$

Using the relation (37) for the components of the Cayley map, this becomes

$$\hat{R}_{h\omega_k}(\mathbf{c}_0)_{k+1} - (\mathbf{c}_0)_k + \hat{\mathbf{x}}_{h\xi_k} = R_{-\theta_k}((\mathbf{c}_1)_{k+1} - (\mathbf{c}_1)_k). \quad (46)$$

Given ω_k , the first component of ξ_k , this relation can be solved to find the corresponding linear velocity \mathbf{v}_k . In fact, since $\hat{\mathbf{x}}_{h\xi_k}$ depends linearly on \mathbf{v}_k , (46) is just a linear equation for \mathbf{v}_k .

Summary. To convince ourselves that the equations derived so far are sufficient to determine the discrete curve g_k , $k = 0, \dots, N$ completely, we summarize the equations of motion. A practical way to implement these equations will be given below in Section 4.3.

Assume that two successive elements $g_{k-1}, g_k \in SE(2)$ are given, which satisfy the admissibility condition (26). The equations allow for g_{k+1} to be found as follows:

1. Using the Cayley transform (36), find $\xi_{k-1} \in \mathfrak{se}(2)$.
2. Solve the following two equations simultaneously for $\xi_k = (\omega_k, \mathbf{v}_k)$: (45) and (46).
3. Given ξ_k and g_k , determine g_{k+1} from the update relation (36).

4.3 Practical Implementation of the Discrete Equations of Motion

Using the projector \mathbb{P} defined in (8), we first write the equations of motion as

$$\mathbb{P}_{(\mathbf{c}_0)_k} \left(-M(\hat{\xi}_k)^T \hat{\mu}_k + M(-\hat{\xi}_{k-1})^T \hat{\mu}_{k-1} \right) = 0 \quad (47)$$

and the boundary conditions as

$$\mathbb{P}_{(\mathbf{c}_0)_0} \left(M(\hat{\xi}_0)^T \hat{\mu}_0 \right) = 0, \quad \text{and} \quad \mathbb{P}_{(\mathbf{c}_0)_N} \left(M(\hat{\xi}_{N-1})^T \hat{\mu}_{N-1} \right) = 0. \quad (48)$$

Here we use the matrix expression $M(\xi)$ for dCay^{-1} , given by (32) and $\hat{\xi}_k = h\xi_k$, $\hat{\mu}_k = h\mu_k$. From now on, we will drop the hat over the linear quantities ξ and μ , as the factors of h in front of ξ and μ can be restored at a later stage without any ambiguity.

The Discrete Equations of Motion for $SE(2)$. We introduce the matrices

$$A(\omega) := \frac{1}{1 + \omega^2/4} \begin{pmatrix} 1 & -\omega/2 \\ \omega/2 & 1 \end{pmatrix}, \quad B(\omega) := A(\omega)^{-1} = \begin{pmatrix} 1 & \omega/2 \\ -\omega/2 & 1 \end{pmatrix}, \quad (49)$$

and observe that

$$M(\xi)^T \mu = \begin{pmatrix} \left(1 + \frac{\omega^2}{4}\right) \pi - \frac{1}{2} \mathbf{p}^T B(\omega) J \mathbf{v} \\ B(\omega)^T \mathbf{p} \end{pmatrix}.$$

Using the fact that $B(\omega)J = J - \frac{\omega}{2}I$, we obtain for the projection (8) that for any point \mathbf{c}

$$\mathbb{P}_{\mathbf{c}}(M(\xi)^T \mu) = \left(1 + \frac{\omega^2}{4}\right) \pi - \frac{1}{2} \mathbf{p}^T J \mathbf{v} + \frac{\omega}{4} \mathbf{p}^T \mathbf{v} + \mathbf{p}^T J \mathbf{c} - \frac{\omega}{2} \mathbf{p}^T \mathbf{c}. \quad (50)$$

Using (40) to write the momenta in terms of ω and \mathbf{v} , we obtain for the projected equation of motion (47)

$$\begin{aligned} m \left(1 + \frac{\omega_k^2}{4}\right) \omega_k + \frac{\omega_k}{4} \|\mathbf{v}_k\|^2 + \mathbf{v}_k^T J(\mathbf{c}_0)_k - \frac{\omega_k}{2} \mathbf{v}_k^T (\mathbf{c}_0)_k \\ = m \left(1 + \frac{\omega_{k-1}^2}{4}\right) \omega_{k-1} + \frac{\omega_{k-1}}{4} \|\mathbf{v}_{k-1}\|^2 + \mathbf{v}_{k-1}^T J(\mathbf{c}_0)_k + \frac{\omega_{k-1}}{2} \mathbf{v}_{k-1}^T (\mathbf{c}_0)_k. \end{aligned} \quad (51)$$

The Linear Velocities. To solve the discrete constraint (46) for \mathbf{v} , we let

$$\mathbf{b}_k := R_{-\theta_k}((\mathbf{c}_1)_{k+1} - (\mathbf{c}_1)_k) - \hat{R}_{\omega_k}(\mathbf{c}_0)_{k+1} + (\mathbf{c}_0)_k, \quad (52)$$

so that (46) is equivalent to $A(\omega_k)\mathbf{v}_k = \mathbf{b}_k$, which can be solved as

$$\mathbf{v}_k = B(\omega_k)\mathbf{b}_k. \quad (53)$$

Notice that the right-hand side depends only on ω_k and θ_k .

The Boundary Conditions. Lastly, we show how the boundary conditions (48) can be made more explicit. We assume that the two discrete curves have been translated to the origin, so that $(\mathbf{c}_0)_0 = (\mathbf{c}_1)_0 = 0$. Using (50), the boundary condition for $k = 0$ becomes

$$\omega_0 \left(m + \frac{1}{4}(m\omega_0^2 + \|\mathbf{v}_0\|^2) \right) = 0,$$

so that $\omega_0 = 0$.

To find \mathbf{v}_0 , we focus on the discrete constraint (46), which becomes for $k = 0$

$$\hat{R}_{\omega_0}(\mathbf{c}_0)_1 + \hat{\mathbf{x}}_{\xi_0} = R_{-\theta_0}(\mathbf{c}_1)_1,$$

so that at $k = 0$, the following conditions hold:

$$\mathbf{x}_0 = 0, \quad \omega_0 = 0, \quad \mathbf{v}_0 = R_{-\theta_0}(\mathbf{c}_1)_1 - (\mathbf{c}_0)_1, \quad (54)$$

and where θ_0 is arbitrary. Once θ_0 is chosen, these relations suffice to find the first two group elements g_0 and g_1 .

At the other end of the curve, the boundary condition (48) for $k = N$ reads

$$m \left(1 + \frac{\omega_{N-1}^2}{4} \right) \omega_{N-1} + \frac{\omega_{N-1}}{4} \|\mathbf{v}_{N-1}\|^2 + \mathbf{v}_{N-1}^T J(\mathbf{c}_0)_N - \frac{\omega_{N-1}}{2} \mathbf{v}_{N-1}^T (\mathbf{c}_0)_N = 0. \quad (55)$$

Summary. To summarize, the discrete equations of motion can be solved as follows. Given an element $(\theta_k, \mathbf{x}_k) \in SE(2)$, we may find the subsequent element $(\theta_{k+1}, \mathbf{x}_{k+1}) \in SE(2)$ by first solving the equations of motion (51) for θ_{k+1} , where ω_k has been eliminated using the Cayley relation (38) and \mathbf{v}_k using the linear relation (53). Afterwards, we then compute \mathbf{x}_{k+1} from θ_{k+1} using the admissibility constraint.

Given an initial condition for θ_0 , the leftmost boundary conditions (54) can be used to find ω_0, \mathbf{x}_0 , and \mathbf{v}_0 . We may then solve the discrete equations in motion to obtain (θ_k, \mathbf{x}_k) for $k = 1, \dots, N$, until we arrive at $k = N$. Starting with arbitrary initial data for θ_0 , the corresponding solution will in general not satisfy the terminal boundary condition (55). Below, we outline a shooting algorithm which will allow us to adjust θ_0 so as to satisfy the terminal boundary condition.

4.4 Solving the Boundary Value Problem

First-Variation Equations. We now solve the boundary value problem (47), (48) using a simple Newton iteration. To this end, we begin by linearizing the equations (51) around a given solution. We denote

$$c_k(\omega, \mathbf{v}) := m \left(1 + \frac{3}{4} \omega^2 \right) + \frac{\|\mathbf{v}\|^2}{4} - \frac{1}{2} \mathbf{v}^T (\mathbf{c}_0)_k$$

and

$$\mathbf{d}_k(\omega) := \frac{\omega}{2} \mathbf{v} + J(\mathbf{c}_0)_k - \frac{\omega}{2} (\mathbf{c}_0)_k.$$

The first-variation equation may then be expressed as

$$c_k(\omega_k, \mathbf{v}_k) \delta \omega_k + \mathbf{d}_k(\omega_k)^T \delta \mathbf{v}_k = c_k(-\omega_{k-1}, -\mathbf{v}_{k-1}) \delta \omega_{k-1} + \mathbf{d}_k(-\omega_{k-1})^T \delta \mathbf{v}_{k-1}. \quad (56)$$

This is a single linear equation for $\delta \omega_k$; $\delta \mathbf{v}_k$ can be obtained from the linearization of (53). After some algebra, we obtain

$$\delta \mathbf{v}_k = J \left(\frac{1}{2} \mathbf{b}_k + A(\omega_k) (\mathbf{c}_0)_{k+1} \right) \delta \omega_k + B(\omega_k) R_{-\theta_k} J((\mathbf{c}_1)_{k+1} - (\mathbf{c}_1)_k) \delta \theta_k,$$

where $A(\omega)$ was defined in (49). Lastly, the variation $\delta \theta_k$ may be obtained from the linearization of the Cayley equation (38) and is given by

$$\delta \theta_{k+1} - \delta \theta_k = \frac{1 - \omega_k^2/4}{1 + \omega_k^2/4} \delta \omega_k.$$

Newton Iteration. Starting with a value θ_{guess} , we set $\theta_0 = \theta_{\text{guess}}$ we solve the equations of motion (51) for $k = 0, \dots, N-1$, and we compute the first variational quantities (56) along the trajectory. At the terminal end of the curve, we compute

$$\delta\theta_{\text{guess}} = \frac{m \left(1 + \frac{\omega_{N-1}^2}{4}\right) \omega_{N-1} + \frac{\omega_{N-1}}{4} \|\mathbf{v}_{N-1}\|^2 + \mathbf{v}_{N-1}^T J(\mathbf{c}_0)_N - \frac{\omega_{N-1}}{2} \mathbf{v}_{N-1}^T (\mathbf{c}_0)_N}{c_N(\omega_{N-1}, \mathbf{v}_{N-1})\delta\omega_{N-1} + \mathbf{d}_N(\omega_{N-1})^T \delta\mathbf{v}_{N-1}};$$

that is, (55) divided by its linearization, and we update θ_{guess} by

$$\theta_{\text{guess}} \mapsto \theta_{\text{guess}} - \delta\theta_{\text{guess}}$$

to obtain our new starting value. The algorithm typically converges to a solution of the boundary value problem after only a few iterations.

5 Direct Minimization of the Energy Functional

Instead of explicitly solving the boundary value problem (47), one can also minimize the deformation energy (39) directly. To bring E into a form which can be handled conveniently by standard optimization software, we write it as

$$hE_0(\theta_0, \dots, \theta_N) = \frac{1}{2} \sum_{k=0}^{N-1} \left(m\omega_k^2 + \|\mathbf{v}_k\|^2 \right). \quad (57)$$

Here, we recall that the linear quantities ω_k and \mathbf{v}_k have been scaled by h ; this explains the factor h in front of E on the left-hand side. Recall that ω_k is given in terms of the angles θ_l by (38), while \mathbf{v}_k is given by (53). Equivalently, E_0 can be written as

$$hE_0(\theta_0, \dots, \theta_N) = \frac{1}{2} \sum_{k=0}^{N-1} \left(m\omega_k^2 + \left(1 + \frac{\omega_k^2}{4}\right) \|\mathbf{b}_k\|^2 \right),$$

where \mathbf{b}_k is given by (52).

The gradient of E_0 with respect to θ_i can easily be computed from this expression. A standard calculation yields

$$\frac{\partial hE_0}{\partial \theta_k} = Q_{k-1} - Q_k + \left(1 + \frac{\omega_k^2}{4}\right) \mathbf{f}_k \cdot \mathbf{g}_k$$

for $k = 1, \dots, N-1$, where

$$Q_i = \left(1 + \frac{\omega_i^2}{4}\right) \left[\left(m + \frac{\|\mathbf{b}_i\|^2}{4}\right) \omega_i - \left(1 + \frac{\omega_i^2}{4}\right) \mathbf{b}_i \cdot \frac{d\hat{R}_\omega}{d\omega}(\omega_i)(\mathbf{c}_0)_{i+1} \right]$$

and

$$\mathbf{f}_i = -\hat{R}_{\omega_i}(\mathbf{c}_0)_{i+1} + (\mathbf{c}_0)_i, \quad \mathbf{g}_i = JR_{-\theta_i}((\mathbf{c}_1)_{i+1} - (\mathbf{c}_1)_i).$$

At the terminal points, we have

$$\frac{\partial hE_0}{\partial \theta_0} = -Q_0 + \left(1 + \frac{\omega_0^2}{4}\right) \mathbf{f}_0 \cdot \mathbf{g}_0 \quad \text{and} \quad \frac{\partial hE_0}{\partial \theta_N} = Q_{N-1}.$$

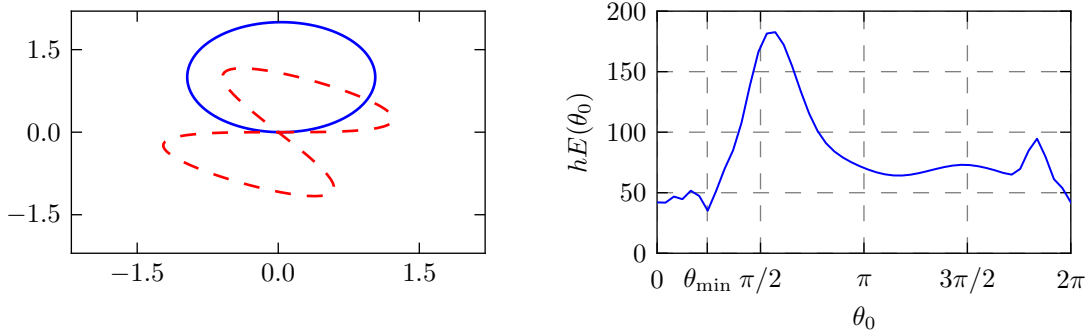


Figure 1: Left: we consider relative geodesics between the circle in blue (solid line) and the figure eight rotated over $\pi/3$ in red (dashed line). Right: the energy as a function of the initial condition θ_0 has several minima. The global minimum is attained for $\theta_{\min} \approx 0.76$, where the energy is approximately 35.12.

N	$\delta(\mathbf{c}_0, \mathbf{c}_1)$
10	<u>37.07641</u>
100	<u>35.12402</u>
1000	<u>35.14675</u>
10000	35.14698

Table 1: Whenever the amount of interpolation points increases by a factor of 10, the accuracy of the discrepancy increases by two digits, suggesting that the order of accuracy of our numerical method is 1.

6 Numerical Results

Unless otherwise noted, the parameter m in the deformation energy (39) will be taken to be equal to 2 in the numerical experiments below.

6.1 Discrepancy of Simple Planar Curves

Relative geodesics between the unit circle and a figure-eight shape. In this example, we compute the discrepancy between the unit circle with parametric representation $\mathbf{c}_0 = (\cos(2\pi s), \sin(2\pi s))$ and the figure eight given by $\mathbf{c}_1(s) = (\sin(4\pi s), \sin(2\pi s))$, for $s \in [0, 1]$. We divide the parameter interval into $N = 100$ equal subintervals, and we let $(\mathbf{c}_i)_k = \mathbf{c}_i(hk)$ for $i = 0, 1$ and $k = 0, \dots, N$, where $h = 1/N$. We finish by rotating and translating both curves so that they start at the origin and are tangent to the x -axis. The final layout of the curves is shown in Figure 1. Upon solving the boundary value problem, we find that the global minimum of the deformation energy is located at $\theta_{\min} \approx 0.7626$, where $\delta(\mathbf{c}_0, \mathbf{c}_1) = E(\theta_{\min}) \approx 35.1236$.

Convergence of the discrepancy. Last, we use the problem of finding the discrepancy between the circle and the figure eight to get a rough estimate of the order of accuracy of our numerical method in terms of the number of sample points on the discrete curves. To do this, we run a number of simulations: at each stage, we choose $N + 1$ sample points on each curve, and we compute the discrepancy between \mathbf{c}_0 and \mathbf{c}_1 . As N increases, the discrepancy is expected to approach a limit value, and the rate at which convergence takes place will give us an estimate of the order of accuracy of our numerical method.

In Table 1, we have listed the discrepancy for a few choices of N . Roughly speaking, as N goes up by a factor of 10, the discrepancy gains two digits of accuracy, so the order of accuracy of the method is approximately one.

6.2 Interpolation for Curves on $SE(2)$

To provide some further visual insight into the nature of relative geodesics, we use a simple form of interpolation on $SE(2)$. Given an element $g \in SE(2)$, we define for $\epsilon \in [0, 1]$,

$$g_\epsilon = \exp(\epsilon \log(g)),$$

where $\exp : \mathfrak{se}(2) \rightarrow SE(2)$ is the exponential map and $\log = \exp^{-1}$ its inverse. The element g_ϵ will be well-defined provided that g is in the range of the exponential map. In this way, we obtain a smooth curve in $SE(2)$ which connects the identity element to g as we let ϵ range from 0 to 1.

Given a curve $s \mapsto g(s)$, we may apply this transformation to each point of the curve in order to obtain a family of curves $g_\epsilon(s)$. Now, assume that the original curve $g(s)$ matches the planar curves \mathbf{c}_0 and \mathbf{c}_1 and set $\mathbf{c}_\epsilon(s) = g_\epsilon(s) \cdot \mathbf{c}_0$. As ϵ ranges from 0 to 1, \mathbf{c}_ϵ will be a curve which smoothly interpolates between \mathbf{c}_0 and \mathbf{c}_1 . A similar procedure may be done for the case of discrete curves.

Most of the computations in the remainder of this section were visualized using the following form of linear interpolation: whenever we compute an admissible curve $g(s)$ with respect to two planar curves \mathbf{c}_0 and \mathbf{c}_1 , we construct the intermediate curves \mathbf{c}_ϵ to give an idea of the deformations carried out by $g(s)$. While the sequence of curves thus obtained has no immediate physical meaning, it nevertheless gives a good intuitive idea of the amount of deformation needed to match one curve with another. To illustrate this, we show in Figure 2 the matching between a circle and a figure-eight shape, where the matching is first done using the global minimizer of the energy (10), and secondly with two different local minimizers.

6.3 Asymmetry of the Discrepancy

We have mentioned before that the discrepancy is not symmetric. We illustrate this by matching a circle \mathbf{c}_0 of radius $r = 0.1$ with a figure-eight shape, given by the parametric representation $\mathbf{c}_1(s) = (\sin(4\pi s), \sin(2\pi s))$. On both curves, 100 points were sampled equidistantly in s , and the parameter m in the norm (10) was set to 2. We find the optimal admissible curve g by means of the algorithm in Section 4.4. For the discrepancy, we obtain

$$\delta(\mathbf{c}_0, \mathbf{c}_1) = 47.6261 \quad \text{and} \quad \delta(\mathbf{c}_1, \mathbf{c}_0) = 39.8011.$$



(a) Global minimum, $\theta_0 = 0.7626$, $E(\theta_0) = 35.1236$.



(b) Local minimum, $\theta_0 = 0.3608$, $E(\theta_0) = 44.4211$.



(c) Local minimum, $\theta_0 = 5.3777$, $E(\theta_0) = 64.9445$.

Figure 2: Matching of a circle and a figure-eight shape using the global minimizer of the deformation energy (Figure (a)) and using two local minimizers (Figures (b) and (c)). The global minimizer deforms the circle into the figure eight with considerably less deformation than the two local minimizers. To indicate the motion of the individual points on the curve, the marks indicate respectively the first point on the curve (circle), the point at index $k = N/3$ (asterisk), and the point at index $k = 2N/3$ (triangle).

The deformations leading to these respective discrepancies are visualized in Figure 3, using the interpolation procedure described in Section 6.2.

As these deformations appear quite similar, despite the large difference in the discrepancies, we investigate some further characteristics of the minimizer. In Figure 4 we plot the θ -coordinate of the minimizer for both matching problems. These curves appear quite different.

6.4 Discrepancy of Polynomial Curves

In this last example, we take a closer look at the relation between discrepancy and other geometrical invariants, in particular the total absolute curvature κ , defined as the integral of

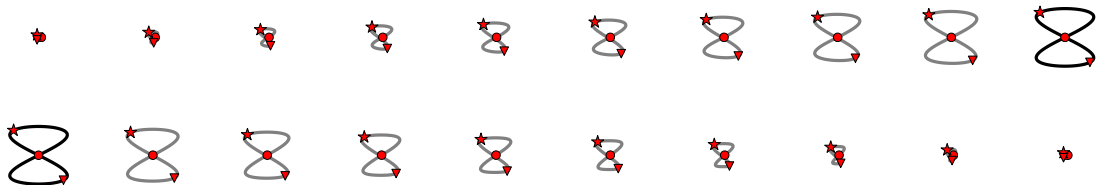


Figure 3: Interpolation between circle and figure-eight (top) and figure-eight and circle (bottom).

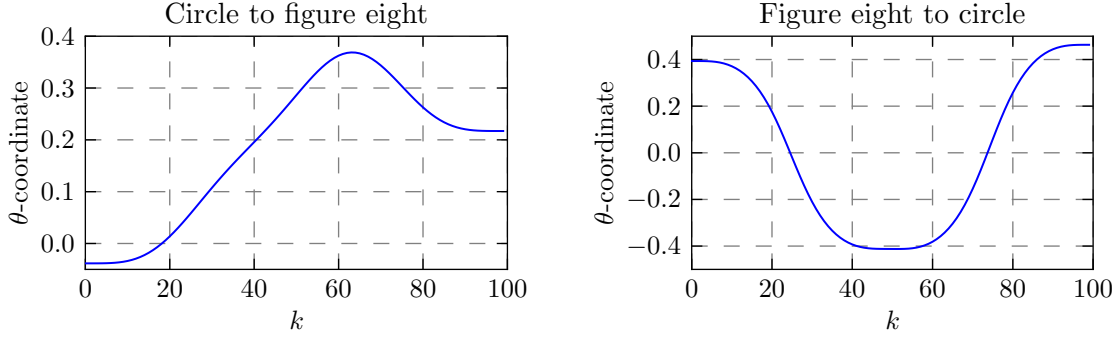


Figure 4: Theta-coordinate for the discrete curve matching the dot to the figure-eight (left), and for the figure-eight matching to the dot (right). These curves are quite different, indicating that the points on the dot, resp. the figure eight, undergo different rotations.

the absolute value of the curvature:

$$\kappa = \int_{s_0}^{s_1} |\rho(s)| ds.$$

We focus on polynomial curves $y = x^p$, for $p = 1, 2, \dots$ and set $\mathbf{c}_p(s) = (x_p(s), x_p(s)^p)$, where the parameter s denotes arclength, $s = 0$ corresponds to the origin, and the curve is traversed in the direction of the positive x -axis (i.e. $x'_p(s) > 0$). Note that the $x_p(s)$ -component is implicitly determined from the equation

$$x'(s) = \frac{1}{\sqrt{1 + p^2 x(s)^{2p-2}}},$$

which can easily be solved for various p by numerical quadrature. We will focus on the unit length segment corresponding to $s \in [0, 1]$. A few of these curves are plotted in Figure 5.

For each of these curves $\mathbf{c}_p(s)$, we choose N equidistant points s_k in the parameter interval $[0, 1]$, so that $s_k = (k - 1)/(N - 1)$ for $k = 1, \dots, N$, and we set $(\mathbf{c}_p)_k = \mathbf{c}_p(s_k)$. In this way, we obtain for each exponent p a discrete curve consisting of N points $(\mathbf{c}_p)_k$, for $k = 1, \dots, N$, at equal distance (along the curve) from each other.

For each exponent $p > 0$, we compute the discrepancy between the discrete curve $(\mathbf{c}_p)_k$ and the fixed curve $(\mathbf{c}_0)_k$, which is parallel to the x -axis. We have tabulated the results for a selection of exponents p in Table 2, along with the total geodesic curvatures for each of the curves \mathbf{c}_p . In Figure 5, both invariants have been plotted for $p = 1, 2, \dots, 25$. We see that the geodesic curvature increases as a function of p , corresponding to the more pronounced bend in the curve for higher p . On the other hand, the discrepancy first increases until $p = 6$ and then decreases: while the curves for high p are more curved, the curvature is more localized and the curves as a whole are close to the x -axis, resulting in lower discrepancy.

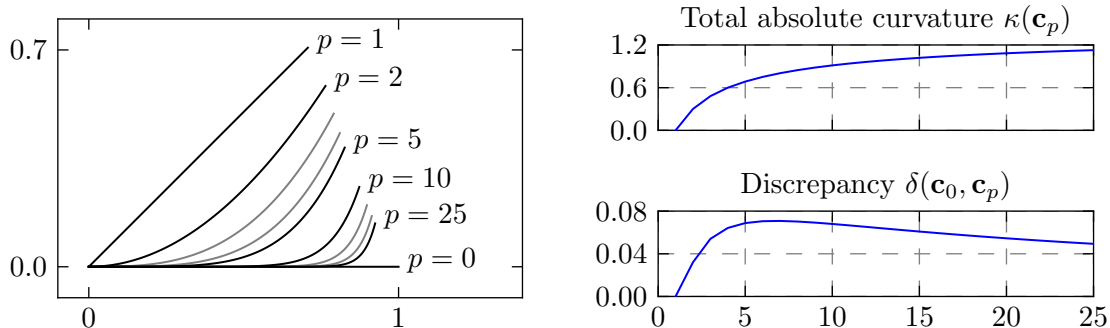


Figure 5: Left: Polynomial curves $\mathbf{c}_p : y = x^p$ for various exponents p . Right: Total absolute curvature of \mathbf{c}_p (top) and discrepancy between \mathbf{c}_0 and \mathbf{c}_p (bottom) as a function of the exponent p . Whereas the total absolute curvature is an increasing function of p , the discrepancy reaches a maximum around $p = 6$ and then decreases.

p	1	2	3	4	5	10	15	20	25
$\delta(\mathbf{c}_0, \mathbf{c}_p)$	0	0.032	0.054	0.064	0.069	0.068	0.061	0.055	0.049
$\kappa(\mathbf{c}_p)$	0	0.301	0.481	0.600	0.685	0.913	1.019	1.083	1.127

Table 2: Table of the discrepancy δ and the total absolute curvature κ for various exponents p . As p increases, the geodesic curvature increases, whereas the discrepancy reaches a maximum value around $p = 5$ and then decreases.

7 Conclusions and Outlook

In this paper, we have outlined a new measure for the discrepancy between planar curves, based on deforming one curve into the other by means of parameter-dependent transformations with values in the Lie group $SE(2)$. We defined a relative geodesic in $SE(2)$ to be a curve of transformations which extremizes a certain energy functional while mapping the first curve into the second, and we defined the discrepancy to be the value of the energy associated to the minimizing relative geodesic.

One of the advantages of our approach is that it can be generalized in a straightforward manner to deal with, for instance, discrepancies and relative geodesics between other types of geometric objects, such as curves in 3D or two-dimensional images. Another direction for future research addresses the choice of Lie group of transformations. In this paper we considered the group $SE(2)$ of rotations and translations, but other groups acting on the plane can be treated similarly. For instance, one could imagine acting on the curves by means of shearing transformations and translations, and in this case the relevant group is the semi-direct product $SL(2)\circledast\mathbb{R}^2$, where $SL(2)$ is the group of 2×2 matrices with unit determinant.

Acknowledgements. We would like to thank Jaap Eldering, Henry Jacobs, and David Meier for stimulating discussions and helpful remarks.

DH and JV gratefully acknowledge partial support by the European Research Council Advanced Grant 267382 FCCA. LN is grateful for support from this grant during a visit to Imperial College. JV is also grateful for partial support by the IRSES project GEOMECH (nr. 246981) within the 7th European Community Framework Programme, and is on leave from a Postdoctoral Fellowship of the Research Foundation–Flanders (FWO-Vlaanderen).

References

- [1] N. Bou-Rabee and J. E. Marsden. Hamilton-Pontryagin integrators on Lie groups. I. Introduction and structure-preserving properties. *Found. Comput. Math.*, 9(2):197–219, 2009.
- [2] H. Cendra, J. E. Marsden, S. Pekarsky, and T. S. Ratiu. Variational principles for Lie-Poisson and Hamilton-Poincaré equations. *Mosc. Math. J.*, 3(3):833–867, 1197–1198, 2003. {Dedicated to Vladimir Igorevich Arnold on the occasion of his 65th birthday}.
- [3] G. S. Chirikjian. *Stochastic models, information theory, and Lie groups. Vol. 1.* Applied and Numerical Harmonic Analysis. Birkhäuser Boston Inc., Boston, MA, 2009. Classical results and geometric methods.
- [4] C. J. Cotter and D. D. Holm. Continuous and discrete Clebsch variational principles. *Found. Comput. Math.*, 9(2):221–242, 2009.
- [5] F. Gay-Balmaz and T. S. Ratiu. Clebsch optimal control formulation in mechanics. *J. Geom. Mech.*, 3(1):41–79, 2011.

- [6] D. D. Holm. *Geometric mechanics. Part II. Rotating, translating and rolling*. Imperial College Press, London, second edition, 2011.
- [7] A. Iserles, H. Z. Munthe-Kaas, S. P. Nørsett, and A. Zanna. Lie-group methods. *Acta Numerica*, 9:215–365, 2000.
- [8] M. Kobilarov. *Discrete Geometric Motion Control of Autonomous Vehicles*. PhD thesis, University of Southern California, 2008.
- [9] M. Kobilarov and J. Marsden. Discrete geometric optimal control on lie groups. *IEEE Transactions on Robotics*, 27(4):641–655, aug. 2011.
- [10] J. Koiller. Reduction of some classical nonholonomic systems with symmetry. *Arch. Rational Mech. Anal.*, 118(2):113–148, 1992.
- [11] J. E. Marsden and T. S. Ratiu. *Introduction to mechanics and symmetry*, volume 17 of *Texts in Applied Mathematics*. Springer-Verlag, New York, 1994.
- [12] D. Mumford and A. Desolneux. *Pattern Theory: The Stochastic Analysis of Real-World Signals*. A. K. Peters, 2010.
- [13] P. J. Olver. *Applications of Lie Groups to Differential Equations*, volume 107 of *Graduate Texts in Mathematics*. Springer-Verlag, New York, 1986.
- [14] A. Stern. Discrete Hamilton-Pontryagin mechanics and generating functions on Lie groupoids. *J. Symplectic Geom.*, 8(2):225–238, 2010.
- [15] D. W. Thompson. *On Growth and Form*. Reprint of 1942 2nd ed. (1st ed. 1917). Dover Publications, 1992.
- [16] H. Yoshimura and J. E. Marsden. Dirac structures in Lagrangian mechanics. II. Variational structures. *J. Geom. Phys.*, 57(1):209–250, 2006.
- [17] L. Younes. *Shapes and diffeomorphisms*, volume 171 of *Applied Mathematical Sciences*. Springer-Verlag, Berlin, 2010.